Electrical Engineering
https://doi.org/10.1007/s00202-019-00791-z

ORIGINAL PAPER

Online generalized droop-based demand response for frequency control in islanded microgrids

Farshid Habibi[1] · **Qobad Shafiee**[1] · **Hassan Bevrani**[1]

Received: 4 January 2019 / Accepted: 21 May 2019

Abstract

Frequency stability, as one of the most important issues in the modern power grids, requires more efficient control methods due to the increasing complexity of the power system, high penetration of distributed generation sources as well as high electrical energy consumption. The challenges become more critical in the case of islanded microgrids (MGs), due to existing no traditional ancillary services of the upstream electric power network. Thus, the modern power grids, such as MGs, need advanced regulation methods to keep the generation-consumption balancing. Demand response (DR) is the recently introduced control approach which guarantees continuous contribution of controllable loads in the system frequency control. In this paper, a new online droop-based DR, generalized droop control (GDC), is introduced to apply in islanded MGs frequency control. An artificial neural network is used for online tuning of droop coefficients in the presented GDC framework. The proposed control approach changes controllable active and reactive loads, using a set of equations based on satisfying dynamics. To evaluate the effectiveness of the proposed control method, several scenarios are simulated in which changes of the system frequency and voltage are studied. Results show significant damping of power–frequency fluctuation and a desirable performance of the closed-loop system.

Keywords Demand response · Droop control · Frequency control · Microgrid · Artificial neural network

1 Introduction

Frequency stability of the power systems is studied in both normal/preventive and off-normal/emergency operating states over the years. In the normal condition, conventional and basic control loops regulate the system frequency, while in the emergency operating state, under frequency load shedding (UFLS), special protection plans and temporary islanding may be used [1, 2]. Making production-consumption balance is an essential control task in all conditions to maintain system performance, network security, reliability, and system efficiency [2]. A common feature of the well-known control methods is a non-continuous contribution of demand side in dynamic regulation. In fact, the contribution of demand side is limited to the temporary emergency conditions.

On the other hand, due to the increasing rate of power consumption, the conventional hierarchical control loops in the generation side may not effectively manage the balance between electrical power production and consumption [3].

Demand response (DR) is a capability of the system to regulate and change consumption of flexible loads based on specified conditions to assure power quality, network security, dynamic performance, and meeting the assigned technical and economic constraints given by the system operators [4]. The DR, as the ability of demand side, can be effectively used to make generation-consumption balance following a serious fault [5]. It has many advantages such as reduction of energy consumption/emission, less power production, and requiring less spinning reserve [6]. Also, domestic vehicles, freezers, and refrigerators are considered as dynamic and flexible loads for the DR [4, 7].

Demand-side participation is often based on centralized and decentralized architectures. In a centralized mode, a

✉ Farshid Habibi
f.habibi@eng.uok.ac.ir

Qobad Shafiee
q.shafiee@uok.ac.ir

Hassan Bevrani
bevrani@uok.ac.ir

[1] Department of Electrical Engineering, Smart/Micro Grids Research Center (SMGRC), University of Kurdistan, Sanandaj, Kurdistan, Iran

Published online: 28 May 2019

central unit processes/monitors the entire system and controls it as well. Network security and inter-communication of many light loads and generation units are the main challenges in the centralized DR process, while in the decentralized method, to meet the mentioned challenges, flexible light loads operate based on the local system frequency/voltage. Hence, a central control unit is unnecessary but it surely needs local smart meters (SMs) which may be very costly. Also, it is often suitable to be used in large-scale systems. A comprehensive review of the DR contribution and conventional frequency control loops is presented in [6, 8, 9]. Since the dynamic of DR is fast, it can impose a quick reaction in the control process. Figure 1 shows the timescale of DR in comparison with other control/protection actions in power systems [10, 11]. In the power network of some countries, the DR contribution has been practically evaluated. The DR is introduced as an alternative option in the power network of Germany, Norway, and Singapore [12–14]. Integration of DR and power generating by wind turbines are analyzed in Germany's electricity market. As a pilot study in Norway, household consumers are considered as a daily DR contributing to peak load shaving. In Singapore, smart residential buildings are studied to establish a mathematical model representing profile models for various types of loads.

Randomized DR for distributed frequency control in smart grids is addressed in [15]. The presented strategy is needless to the centralized controllers, and complex communication networks due to the system and loads are flexible/controllable. The system frequency is exclusively regulated by the proposed algorithm without the conventional frequency controllers. In some studies, the frequency thresholds are used for connecting/disconnecting loads contributing to the DR algorithm [11, 16, 17]. In [13, 18–21], the DR contributes in the dynamic regulation of the MG systems containing distributed generations (DGs) and renewable energy sources (RESs). In these studies, the DR is introduced to the power system as a contributor in the primary frequency control loop. Due to the regular availability of smart loads in the modern power systems, the DR can be considered as a spinning reserve capacity [22–25]. Other aspects of the DR such as economic advantages are surveyed in [12, 13, 26].

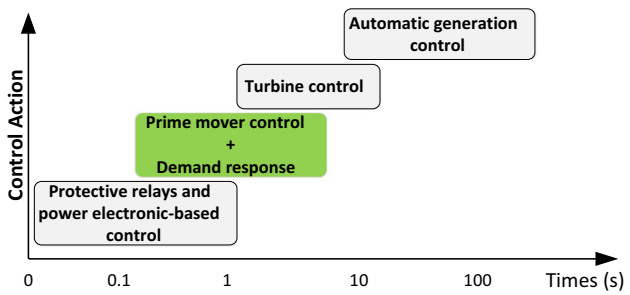

Fig. 1 The timescale of DR comparing the other control loops

The modern power networks need advanced regulation methods to keep the generation-consumption balancing. This is going to be more important due to the increasing number of MGs, varying structure, environmental concerns, and complication of power networks. Besides the MG systems, a number of synchronous generators in power systems are going to be replaced by RESs and DGs such as microturbines, photovoltaic panels, wind turbines, energy storage systems, fuel cells, and reciprocating engines [27]. Therefore, the inertia of the entire system is significantly reduced and this degrades the system stability following different disturbances [28, 29]. In many applications, energy storage systems are used to preserve the system stability, following fault occurrences. However, the capacity of DGs and RESs, as main production units in MGs, are limited. These limitations and uncertainties introduce DR as an appropriate solution choice to provide a dependable, low cost, eco-friendly power grid [30].

In the present paper, an adaptive mechanism is proposed to use the controllable loads in the regulation process. The salient features of the proposed intelligent methodology are as follows.

- A mathematical model for a generalized droop control (GDC)-based DR is represented.
- To solve the practical problems of GDC-based DR approach in a wide range of operating points, an intelligent online GDC-based DR is introduced.
- Artificial neural network (ANN) is employed for online tuning of GDC droop coefficients. The method smartly uses flexible loads to keep frequency stability, while it simultaneously regulates the voltage profile as well.
- The proposed method is applicable for the various scale of power grids operating in different conditions.

The rest of this paper is organized as follows. Section 2 provides an overview of the DR coordination with frequency control loops in modern power systems. The proposed control framework is described in Sect. 3. A MG test system is considered to verify the effectiveness of the proposed control scheme in Sect. 4. Section 5 concludes the paper.

2 Coordination of DR and conventional frequency control loops

In the generation side of power systems, there are primary, secondary, and tertiary frequency control loops proceeding to regulate system frequency. While, in the demand side, the UFLS is only used as frequency control in emergency conditions (emergency control loop).

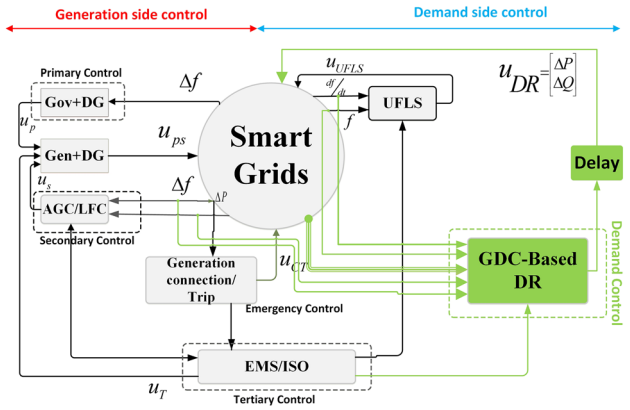

Fig. 2 The updated frequency control loops in modern power systems

In the presence of DR, frequency control loops can be updated as shown in Fig. 2. In addition to the conventional frequency control loops [2, 31], the DR loop can be realized in the demand side. The DR-based frequency control loop is a continuous control action that supports system regulation, operation, and marketing issues. The DR algorithm may have various inputs such as system frequency (f) and voltage (V), changes of system frequency (Δf) and voltage (ΔV), power deviations (ΔP, ΔQ). It may receive some commands from the upstream units like energy management system/ independent system operator (EMS/ISO). The EMS/ISO can specify certain thresholds for operating point of existing frequency control loops. It also sends the necessary information to the DR loop including network status, power consumption, quantity of the available controllable loads, and market conditions. In fact, EMS/ISO monitors the existing control loops in both generation and demand sides.

The DR command signal (U_{DR}) after a time delay (about 0.1 s) due to the computations and communication channels [16, 32] is finally applied to the determined controllable loads in demand side. The proposed control is implemented in MG central control (MGCC) and realized through the secondary control level.

Depending on the conditions, the proposed method may partially or fully share the flexible loads in the DR process. This contribution, which is based on a regular planning, can significantly reduce the UFLS. The removed/changed controllable active/reactive loads (smart loads) will be reconnected to the network, later in the normal operating state. These control–protection processes must be done in a perfect harmony with distribution companies and consumers.

3 Proposed control framework

In this section, an intelligent DR-based control is introduced. First, the well-known power equations for the generation side and the conventional droop control relationship are represented. Then, a generalized form of droop control is obtained. Using these equations, a generalized model for DR-based control is presented.

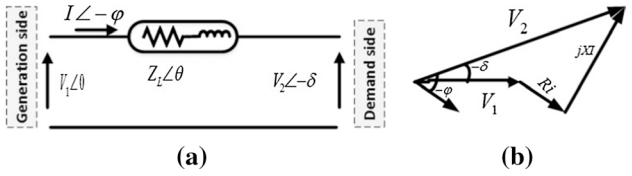

Fig. 3 Transmission line between generation side and demand side: **a** power line, **b** phasor diagram

3.1 Droop characteristic-based power control

The power equations of a transmission line, as represented in Fig. 3, can be written as:

$$S_L = P_L + jQ_L = V_1 I^* = V_1 \left(\frac{V_1 - V_2}{Z_L} \right)^* = V_1 \left(\frac{V_1 - V_2 e^{j\delta}}{Z_L e^{-j\theta}} \right) = \frac{V_1^2}{Z_L} e^{j\theta} - \frac{V_1 V_2}{Z_L} e^{j(\theta+\delta)} \tag{1}$$

where $S, P, Q, V_1, V_2, Z, \theta$ and δ are apparent power, active power, reactive power, primary side voltage, demand-side voltage, line impedance, the angle of impedance and angle of load-side voltage, respectively. The active and reactive power transmitting through the line are:

$$P_L = \frac{V_1^2}{Z_L} \cos\theta - \frac{V_1 V_2}{Z_L} \cos(\theta + \delta) \tag{2}$$

$$Q_L = \frac{V_1^2}{Z_L} \sin\theta - \frac{V_1 V_2}{Z_L} \sin(\theta + \delta) \tag{3}$$

Considering $Z_L e^{j\theta} = R_L + jX_L$, (2) and (3) can be rewritten as

$$P_L = \frac{V_1}{R_L^2 + X_L^2} [R_L (V_1 - V_2 \cos\delta) + X_L V_2 \sin\delta] \tag{4}$$

$$Q_L = \frac{V_1}{R_L^2 + X_L^2} [-R_L V_2 \sin\delta + X_L (V_1 - V_2 \cos\delta)] \tag{5}$$

where R_L and X_L are resistance and reactance of the line. Equations (4) and (5) are based on the basic parameters of line and can be stated as

$$V_2 \sin\delta = \frac{X_L P_L - R_L Q_L}{V_1} \tag{6}$$

$$V_1 - V_2 \cos\delta = \frac{R_L P_L + X_L Q_L}{V_1} \tag{7}$$

For the systems with $X_L \gg R_L$, power angle δ is small and R is negligible. Thus, (6) and (7) can be simplified as

$$\delta \cong \frac{X_L P_L}{V_1 V_2} \tag{8}$$

$$V_1 - V_2 \cong \frac{X_L Q_L}{V_1} \tag{9}$$

Above relationships describe that δ is mainly depended on P_L and, $V_1 - V_2$ depends on Q_L. Dynamically, frequency regulation controls δ and subsequently regulates P_L. Also, voltage regulation controls Q_L. Accordingly, the following well-known droop characteristic equations are defined where k_p and k_q are droop coefficients of frequency–active power and voltage–reactive power, respectively.

$$f_{\text{grid}} - f_0 = -k_P \left(P_{\text{grid}} - P_0\right) \tag{10}$$

$$V_{\text{grid}} - V_0 = -k_q (Q_{\text{grid}} - Q_0) \tag{11}$$

In fact, the droop-based system frequency–voltage regulation as a traditional way is reported in many studies [17, 33–37]. Hence, Eqs. (10) and (11) are the well-known frequency/voltage droop regulation forms, where $X >> R$.

In the mathematical models of systems such as MGs, both X_L and R_L should be considered to improve accuracy of the system modeling. In such networks, a transformation matrix T can be used to convert P_L and Q_L in (4) and (5) to modify P'_L and Q'_L, respectively, i.e.,

$$\begin{bmatrix} P'_L \\ Q'_L \end{bmatrix} = T \begin{bmatrix} P_L \\ Q_L \end{bmatrix} = \begin{bmatrix} \sin\theta & -\cos\theta \\ \cos\theta & \sin\theta \end{bmatrix} \begin{bmatrix} P_L \\ Q_L \end{bmatrix} = \begin{bmatrix} \frac{X_L}{Z_L} & -\frac{R_L}{Z_L} \\ \frac{R_L}{Z_L} & \frac{X_L}{Z_L} \end{bmatrix} \begin{bmatrix} P_L \\ Q_L \end{bmatrix} \tag{12}$$

Applying the transformation matrix T and some substitutes, a generalized form of droop characteristic can be found as follows [37]:

$$f_{\text{grid}} - f_0 = -k_p \left(P'_L - P'_0\right) = -k_p \frac{X_l}{Z_L} \left(P_L - P_0\right) - k_p \frac{R_L}{Z_L} \left(Q_L - Q_0\right) \tag{13}$$

$$V_{\text{grid}} - V_0 = -k_q \left(Q'_L - Q'_0\right) = -k_q \frac{R_L}{Z_L} \left(P_L - P_0\right) - k_q \frac{R_L}{Z_L} \left(Q_L - Q_0\right) \tag{14}$$

Equations (13) and (14) demonstrate that frequency and voltage deviations in MGs systems are depended on both active and reactive power changes. In such systems, both active and reactive power must be monitored/controlled simultaneously to regulate system frequency and voltage. Instead of high inertia power plants, the DGs and RESs are available in MGs, and this causes dynamic oscillations in the face of disturbances. It more critically occurs in the islanded MGs.

The conventional and generalized droop characteristic are found to use in the generation side of the power systems. In the next step, the generalized droop characteristic is adapted to apply in the demand side of an isolated MG.

3.2 Developed GDC-based DR

In most of published works, the conventional form of droop characteristics, i.e., (10) and (11), has been considered for DR [12, 13, 20, 22]. This seems to be an inappropriate methodology for the power electronics-based systems like MGs, where no more overhead lines exist. This challenge is more critical for islanded MGs. Therefore, a modified/generalized form of DR is needed for the MG systems.

From the GDC equations of the generation side, i.e., (13) and (14), one can use them as control laws for frequency and voltage regulation. Therefore, Δf and ΔV can be written as functions of ΔP_L and ΔQ_L.

$$\begin{cases} \Delta F = F(\Delta P_L, \Delta Q_L) \\ \Delta V = U(\Delta P_L, \Delta Q_L) \end{cases} \tag{15}$$

Since the DR methods are presented for the demand side, Δf and ΔV are input signals and ΔP_L and ΔQ_L are the target signals. Hence, in this mode, one can find ΔP_L and ΔQ_L based on Δf and ΔV as given in (16).

$$\begin{cases} \Delta P_L = f_P(\Delta f, \Delta V) \\ \Delta Q_L = f_Q(\Delta f, \Delta V) \end{cases} \tag{16}$$

To find (16), (13) and (14) are rewritten as

$$\begin{bmatrix} -k_p \frac{X_L}{Z_L} & -k_p \frac{R_L}{Z_L} \\ -k_q \frac{R_L}{Z_L} & -k_q \frac{R_L}{ZL} \end{bmatrix} \begin{bmatrix} \Delta P_L \\ \Delta Q_L \end{bmatrix} = \begin{bmatrix} \Delta F \\ \Delta V \end{bmatrix} \tag{17}$$

The proposed GDC-based DR algorithm is found based on the given formula in (18). It is able to compute the amount of smart loads (SLs) contributing in the DR algorithm. The SLs are found in smart homes (SHs) which are monitored/controlled via the network in response to the dynamic regulation.

$$g(\Delta f, \Delta U) = \begin{bmatrix} -\frac{Z(\Delta V \cdot k_p \cdot R + \Delta F \cdot k_q \cdot X)}{k_p \cdot k_q (R^2 + X^2)} \\ \frac{Z(\Delta F \cdot k_q \cdot R - \Delta V \cdot k_p \cdot X)}{k_p \cdot k_q (R^2 + X^2)} \end{bmatrix} = \begin{bmatrix} \Delta P_L \\ \Delta Q_L \end{bmatrix} \tag{18}$$

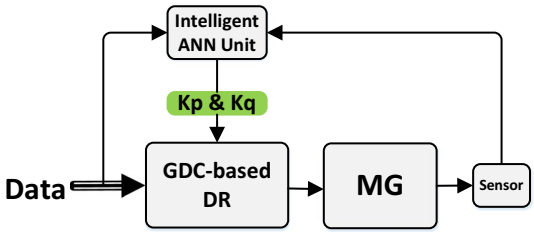

Fig. 4 The general schematic for online tuning of droop coefficients

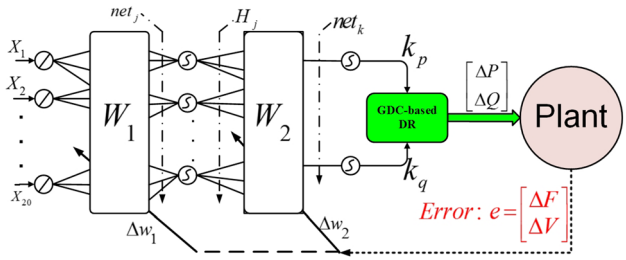

Fig. 5 ANN structure to adjust droop coefficients of the proposed GDC

Using (18), the GDC-based DR can be applied to any system including the MG systems.

3.3 Online GDC-based DR

The mathematical model of the GDC-based DR is given in (18) where its performance is strongly dependent on the values of k_p and k_q. The conventional methods in [17, 35] adjust k_p and k_q for a particular condition. When operational conditions of the system change or a severe disturbance occur, the set values will not be optimal. Thus, an online tuning of k_p and k_q can be a good solution to address the mentioned challenge.

The ANN as a powerful tool is an appropriate choice to achieve the proposed control goals [38, 39]. General ANN-based structure for online tuning of k_p and k_q is shown in Fig. 4. As seen, input signals of the ANN-based intelligent unit are containing the MG output and a set of basic data. The intelligent unit collects initial required data, and subsequently proceeds to generate k_p and k_q that are used by the GDC-based DR unit to compute ΔP_L and ΔQ_L commands. The MG receives the command signals considering a time delay caused by the communication network. Detail of the proposed method is given in Fig. 5.

The number of neurons for input and hidden layers is selected based on the prior knowledge considering system conditions. In case of high number of input neurons, there is a possibility of divergence, while the best performance may not be achieved with a low number. Also, the required outputs determine the number of output neurons. Therefore, the proposed ANN is considered by 20 input neurons, 10 neurons in the hidden layer, and 2 neurons for the output layer. X, W_1, and W_2 are inputs vector, and weight vector of first and second layers, respectively.

Appropriate selection of the initial conditions directly affects the ANN performance and, it is set based on the prior knowledge of the ANN and the system conditions. Hence, the input vectors are initialized as follows:

$$\begin{cases} X = ones\,(20, 1) \\ W_1 = rand\,(10, 20) \\ W_2 = rand\,(2, 10) \end{cases} \tag{19}$$

One of the important advantages of the nonlinear function-based neurons is smoothly updating the weights. It causes no sudden jumps in the weights update. Therefore, the sigmoid functions are selected for hidden and output layers as shown in Fig. 5. The learning process for online tuning of k_p and k_q is based on minimizing

$$J = \frac{1}{2}\sum_{i=1}^{n}(y_{di} - y_i^m)^2 \tag{20}$$

where y_d and y^m are desirable/reference value and measured output, respectively. The weights are updated by the back-propagation (BP) method. As a powerful learning method, it can be used in a wide range of applications and has several outstanding features including the high representation power, the wide applicability of BP learning, easy to implement, and proper generalization power [40, 41].

In the feed-forward process, outputs of the hidden layer (H_j) and the output layer (net_k) are prepared as shown in Fig. 5. Also, the error vector is collected as:

$$\text{Error} = \begin{bmatrix} \Delta F \\ \Delta V \end{bmatrix} \tag{21}$$

In the feedback process, the weights are updated as follows:

$$\begin{cases} w_2(k+1) = w_2(k) + \Delta w_2 \\ w_1(k+1) = w_1(k) + \Delta w_1 \end{cases} \tag{22}$$

where Δw_1 and Δw_2 are the weights found based on the BP learning method [42]. Detail of the proposed control framework is given in the flowchart of Fig. 6.

The proposed online GDC-based DR centrally manages the demand-side contribution. The considered ANN is trained by the response for a set of different scenarios and based on the system dynamics to online prepare the droop coefficients (Kp and Kq). These coefficients as the input signals are used by the GDC-based DR algorithm, as shown in Fig. 4.

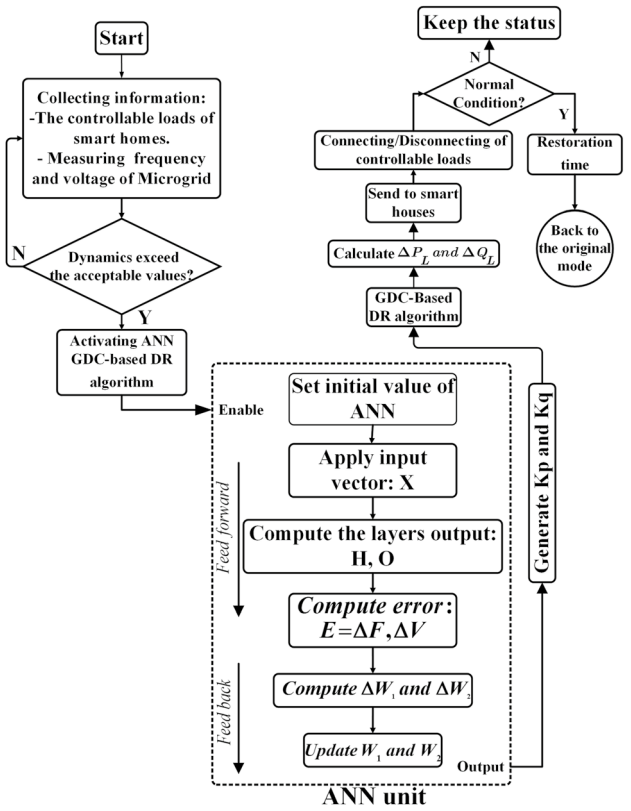

Fig. 6 Flowchart of the proposed online GDC-based DR

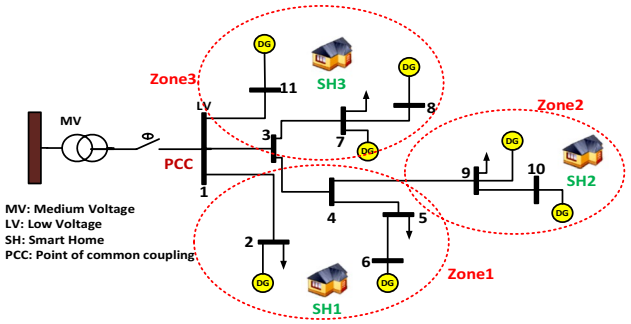

Fig. 7 The MG test system

Table 1 Specifications of loads in the zones

Zone 1	Controllable loads	10 kW	4 kVar
	Non-controllable loads	$45+j5$ (kVA)	
Zone 2	Controllable loads	15 kW	7 kVar
	Non-controllable loads	$40+j20$ (kVA)	
Zone 3	Controllable loads	5 kW	2 kVar
	Non-controllable loads	$20+j10$ (kVA)	

It should be noted that the proposed online GDC-based DR algorithm as a new control loop of the demand side is used with the conventional control loops of the generation side for the system frequency/voltage regulation, as conceptually shown in Fig. 2.

4 Simulation results

To evaluate the effectiveness of the proposed control method, an 11-bus distribution system is considered as an isolated MG [44]. The single-line diagram of the test system is shown in Fig. 7. The MG test system has three zones containing DG units, a smart home and local loads. The controllable loads located in the smart homes can be used by the proposed control method.

The specifications of loads in the zones are listed in Table 1. Since, the MG systems are often small scale, the behavior of its dynamics is similar in all buses, a centralized DR mode has been considered to apply the proposed control methodology. Hence, an SM is located on the PCC, shown in Fig. 7, to collect/measure ΔF and ΔV to be processed by the online GDC algorithm. Subsequently, it determines the amount of required DR following different disturbances [43]. The smart homes are capable of interrupting, connecting, and changing the controllable loads by data received via the network. Typical controllable and non-controllable loads of zone 1 are given in Table 2.

Providing the controllable active/reactive loads from typical domestic loads is the main challenge of the DR approach. A domestic vehicle can be contributed to the DR algorithm while connecting/disconnecting to/from the network is harmless to the consumers. Accordingly, air conditioners, dishwashers, washing machines and so on (Table 2) can be commanded via the proposed GDC-based DR. To provide such controllable loads, the loads must be equipped with special controllable equipment.

Several domestic vehicles are considered as contributors of Zone 1 in DR algorithm, given in Table 2. As an example, the active and reactive power consumptions of air conditioner are, respectively, 1500 [W] and 600 [Var]. Disconnecting this load via the network, and in response to the system conditions, creates a controllable capacity in size of 1500 [W] and 600 [Var]. In result, each controllable load has a certain controllable capacity. Thus, the controllable active and reactive capacities of Zone 1 are totally 10 [kW] and 4 [kVar], respectively.

The controllable active/reactive loads are distributed in the MG system. As described, a centralized DR algorithm is considered due to the MG systems conditions. The management of each controllable load needs a costly SM and an intelligent decision-making unit. Therefore, the MG system is divided into three zones, to the study be affordable. In other words, the output signal of the online GDC-based DR unit manages the required demand-side

Table 2 Specification of zone 1

			Appliances	Rated power (VA)
Zone 1	Controllable loads	10 + *j*4 (kVA)	Air conditioner	1500 + *j*600
			Dishwashers	1500 + *j*600
			Washing machine	1500 + *j*600
			Heating coil	2000 + *j*800
			Water heater	2000 + *j*800
			Refrigerator	1500 + *j*600
	Non-controllable loads		45 + *j*5 (kVA)	

contribution following different disturbances. Based on the available controllable loads of each zone, given in Table 1, the required contribution is shared between the zones.

To show the performance of the proposed method, several scenarios are studied where the frequency and voltage dynamics are compared considering the following three control modes.

Case 1 Only conventional controllers (CCs) in the local and supplementary levels of generation side are operating.

Case 2 In addition to the CC, the GDC-based DR contributes (GDC-based DR + CC) while the droop coefficients are set by the conventional method. Conventionally, the droop coefficients are designed according to the acceptable range of frequency/voltage per maximum generated active/reactive powers [17, 35]. This means, for a step load of $\Delta P_L + j\Delta Q_L$, the droop coefficients are calculated as

$$\begin{cases} k_p = -\frac{\Delta F}{\Delta P_L} \\ k_q = -\frac{\Delta V}{\Delta Q_L} \end{cases} \tag{23}$$

For a step load of $10 + j5$ (kVA), k_p and k_q are set as depicted in Fig. 8.

Case 3 Case 2 is repeated while k_p and k_q are updated online by the proposed ANN (online GDC-based DR).

4.1 Performance assessment under a DG unit outage

In the first scenario, a DG unit of 100 [kW] is suddenly interrupted at $t = 0.3$ s. In the presence of three control methods, the system frequency and voltage subjected by the disturbance are carried out and the results are depicted in Fig. 9. Considering the results, it can be seen that ΔF and ΔV are reduced by the proposed control method. Figure 9c, d shows the proper contribution of the smart active and reactive loads of MG, in the presence of online GDC-based DR. This performance improvement is a result of online tuning of k_p and k_q shown in Fig. 9e, f.

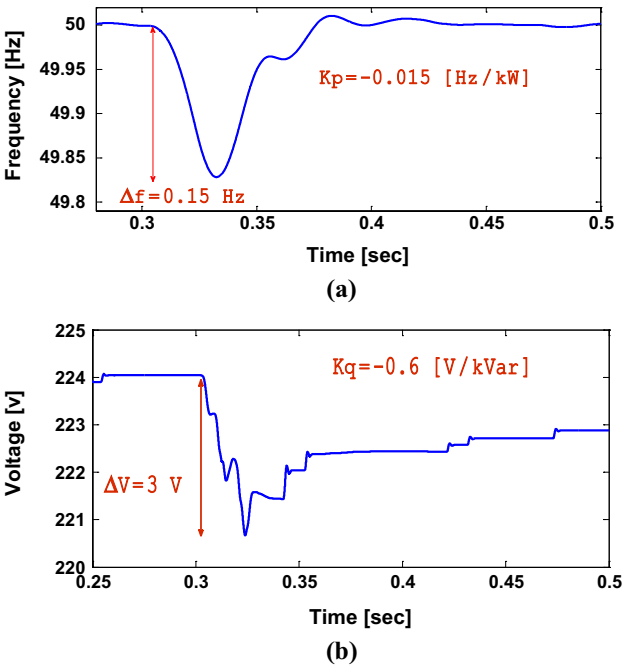

Fig. 8 Finding droop coefficients based on (19): **a** *Kp*, and **b** *Kq*

4.2 Performance assessment under a step load disturbance

In the second scenario, a step load disturbance of $10 + j5$ (kVA) is applied to the test system at $t = 0.3$ s and results are depicted in Fig. 10. In the case of comparing the performance of different control modes, the system frequency and voltage are given in Fig. 10a, b. The smart loads participate in the proposed DR algorithm as shown in Fig. 10c, d representing a continuous contribution of DR in dynamic regulation. The online GDC-based DR can ensure an appropriate performance: the system frequency and voltage dynamics are well-regulated comparing the other two controllers.

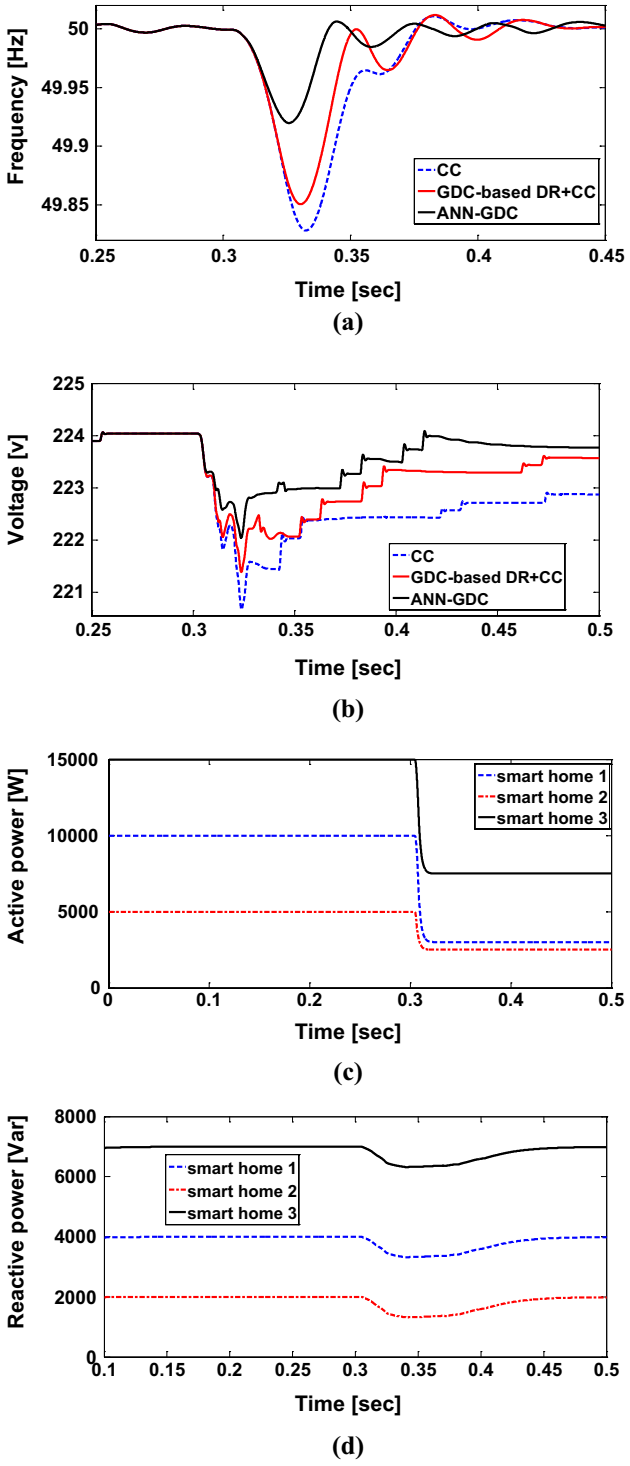

Fig. 9 Performance of the proposed control approach under a DG outage: **a** system frequency, **b** system voltage. **c** Active load change based on the third control mode, **d** reactive load change, **e** generated *kp* by ANN, and **f** generated *kq* by ANN

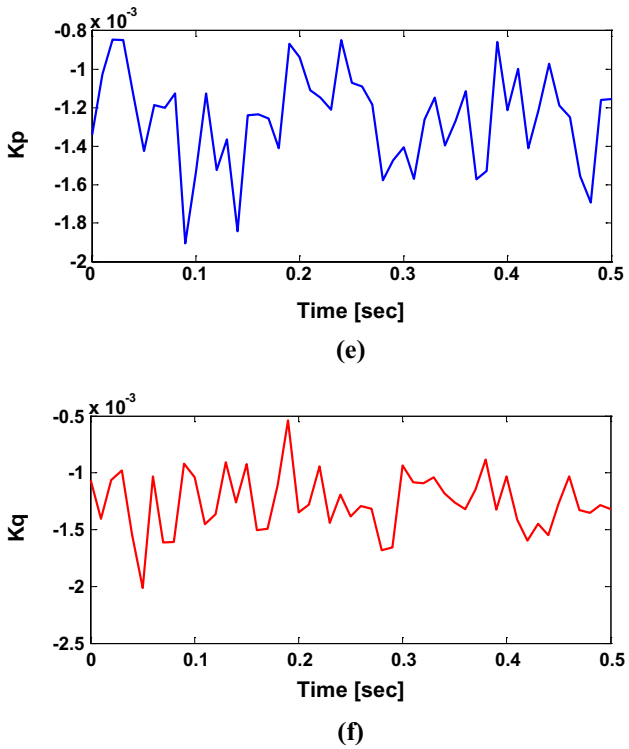

Fig. 9 (continued)

4.3 Performance assessment under a severe disturbance

The proposed controller's performance is studied under severe disturbances. Both step load disturbance and DG unit outage have simultaneously occurred at $t = 0.3$ s. Subjected by this event, frequency and voltage of the MG system are carried out and, depicted in Fig. 11. As shown, the first and second control methods are unable to stabilize the system frequency and voltage. It may lead to activating the frequency relays, and even the possibility of blackout exists. However, the online GDC-based DR can regulate the system frequency and voltage by the continuous and optimal contribution of controllable active and reactive loads.

4.4 General test of the proposed control method

The X/R as an important index determining the type of power systems. In the transmission systems,$X \gg R$, while in distribution systems like MGs both X and R are influential variables. As mentioned in Sect. 3, the proposed control method can be utilized for power networks with different X/R. Here, as a new scenario, the generality of the online GDC-based DR is evaluated by studying the impacts of

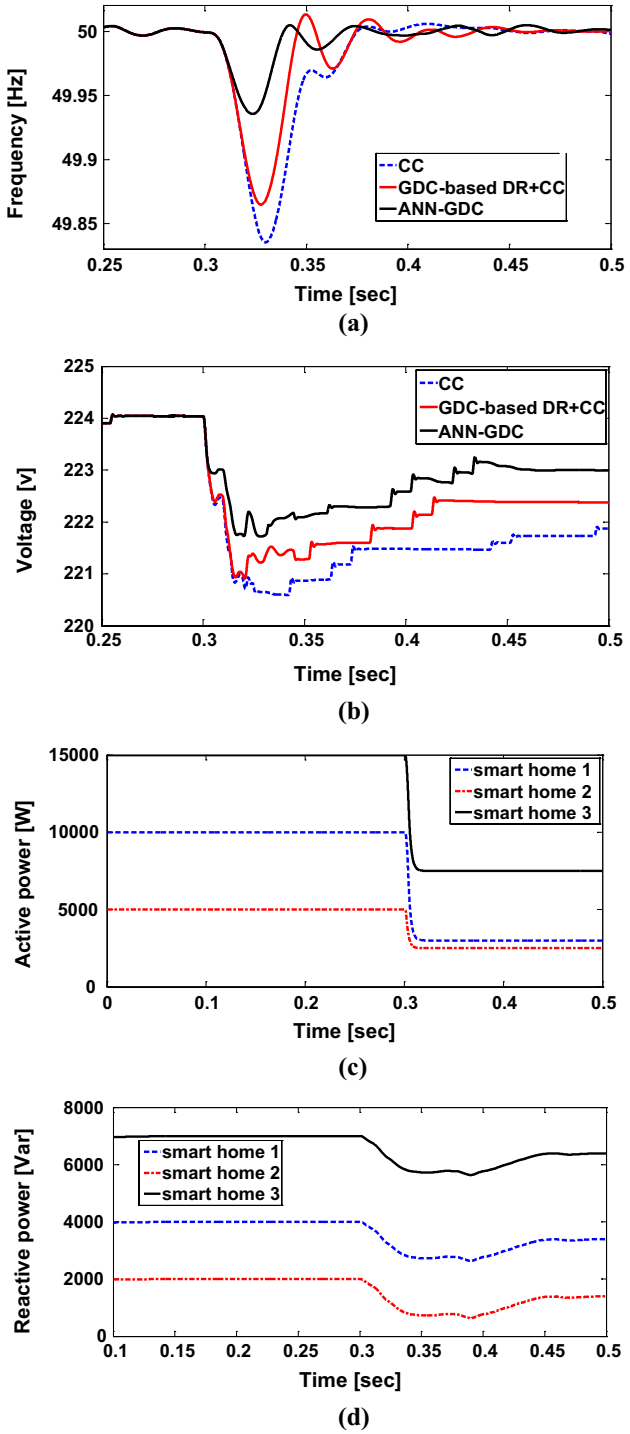

Fig. 10 Performance of the proposed control approach under step load change: **a** system frequency, **b** system voltage, **c** controllable active load change based DR, and **d** controllable reactive load change based DR

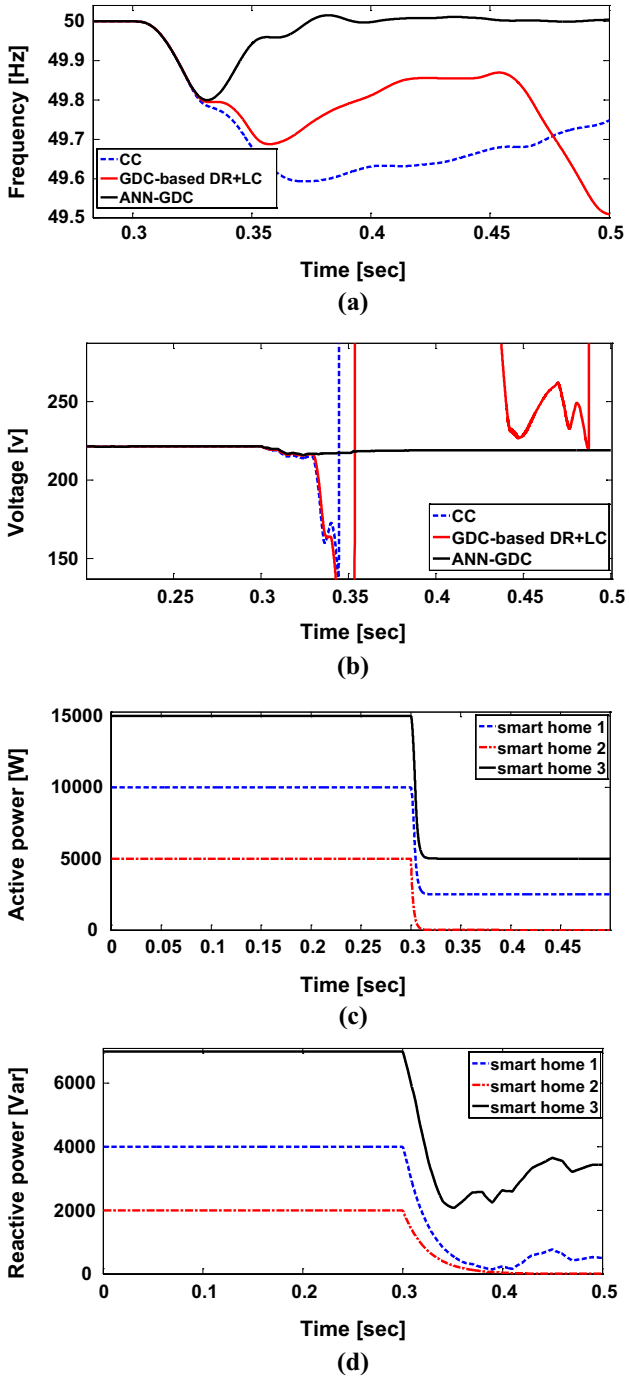

Fig. 11 Impacts of A DG unit outage and step load change simultaneously: **a** system frequency, **b** system voltage, **c** controllable active load change, and **d** controllable reactive load change

X/R. Therefore, *Scenario B* is repeated in the state of $X=R$, $X=5R$, $X=10R$, and $R=5X$. The frequency and voltage profiles are plotted in Fig. 12a, b. According to the results, the proposed control methodology can effectively control the frequency and voltage in the all state.

4.5 Quantitative evaluation of the control methods

Proper performance of the proposed control method is qualitatively observed using several simulation scenarios. Moreover, here for quantitative evaluation of the control modes, performance indices are defined as given in (24) where T,

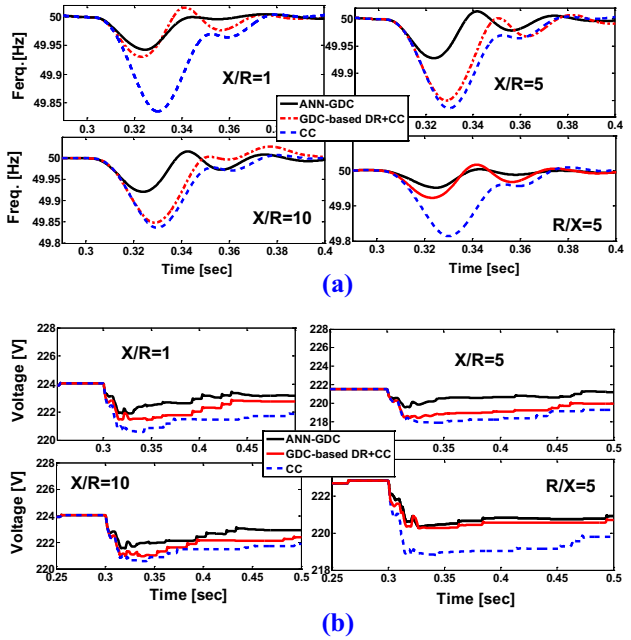

Fig. 12 Impact of X/R ratio on the GDC-based DR performance: **a** system frequency, and **b** system voltage

Table 3 Numerical results of $\int_0^T |\Delta F|^2 \mathrm{d}t$

Scenarios	Controller		
	Conventional controller (CC)	GDC-based DR + CC	Online GDC-based DR + CC
Scenario A	0.0005864	0.0004053	9.271×10^{-5}
Scenario B	0.0005202	0.0003486	5.132×10^{-5}
Scenario C	Instable	Instable	0.0007512

Table 4 Numerical results of $\int_0^T |\Delta V|^2 \mathrm{d}t$

Scenarios	Controller		
	Conventional controller (CC)	GDC-based DR + CC	Online GDC-based DR + CC
Scenario A	1.339	0.9254	0.4798
Scenario B	2.596	1.956	1.047
Scenario C	Instable	Instable	3.953

ΔF and ΔV are simulation time, frequency deviation, and voltage fluctuations, respectively. The performance indices are calculated for described simulation scenarios giving in Tables 3 and 4. Numerical results illustrate that the online GDC-based DR provides a superior performance.

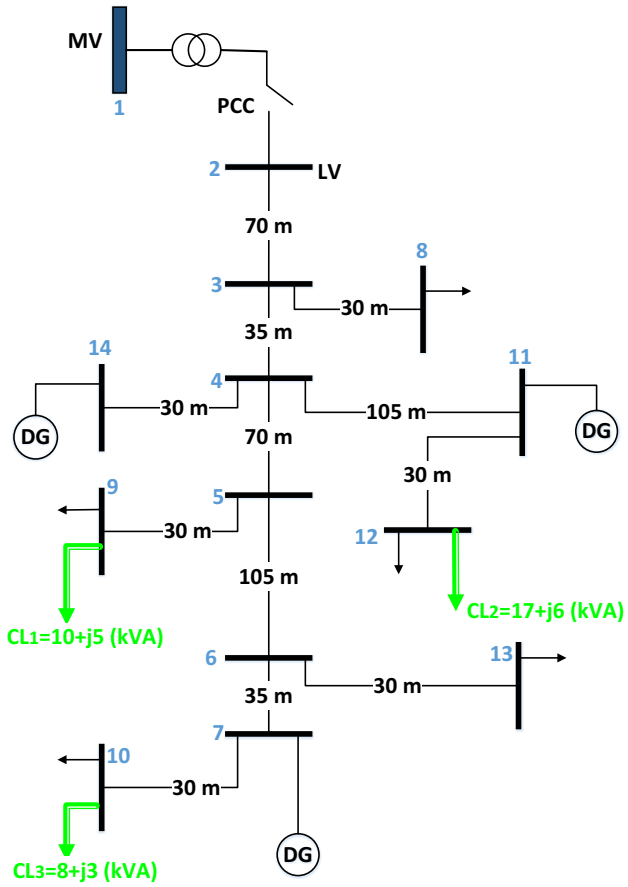

Fig. 13 The IEEE 14-bus distribution system

$$\begin{cases} \int_0^T |\Delta F|^2 \mathrm{d}t \\ \int_0^T |\Delta V|^2 \mathrm{d}t \end{cases} \tag{24}$$

4.6 The effectiveness evaluation of the control method in IEEE 14-bus distribution system

For a more accurate evaluation and an additional example, the effectiveness of the proposed control method is checked in an IEEE 14-bus distribution system, as well. The detail of this test system is reported in [44]. As shown in Fig. 13, three controllable loads are considered to contribute to the proposed control method. Subjected by a step load disturbance of $10+j5$ (kVA) at $t=0.3$ s, and system frequency and voltage are depicted in Fig. 14a, b. Also, the contribution of controllable active and reactive loads in the proposed control approach, is, respectively, shown in Fig. 14c, d. The simulation results illustrate that the proposed control method can present a proper performance in this scenario, as well.

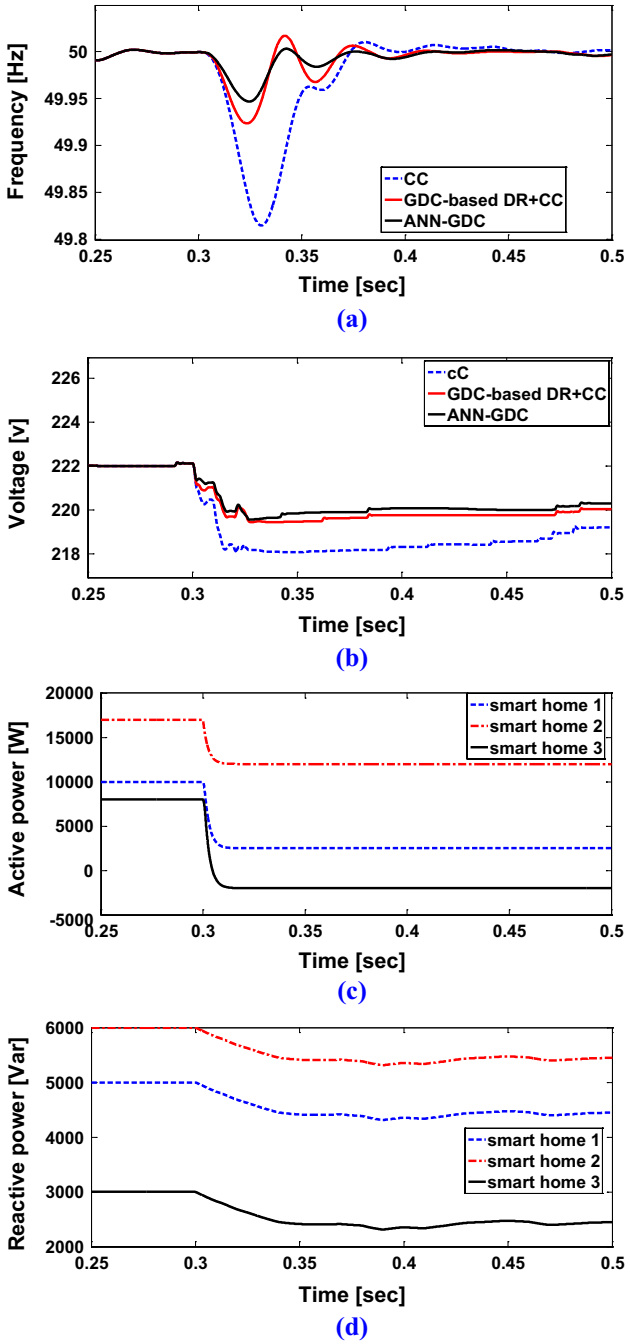

Fig. 14 Performance of the proposed control approach under step load disturbance in the IEEE 14-bus distribution system: **a** system frequency, **b** system voltage, **c** controllable active load change based DR, and **d** controllable reactive load change based DR

5 Conclusion

This paper introduces an intelligent method to contribute the demand side in the DR algorithm supporting frequency and voltage regulation in islanded MGs. A model is presented for DR methodology based on the well-known generalized droop control. However, the presented model depends on the MG conditions as well as the values of droop coefficients. In response to this challenge, an online GDC-based DR is introduced. The proposed approach updates the droop coefficients of the GDC-based DR using online ANN. Performance of the proposed control approach is evaluated using an 11-bus and IEEE 14-bus distribution systems. Several scenarios are simulated under different disturbances. The results illustrate that the online GDC-based DR provides an appropriate performance such that the frequency deviations and voltage variations exposed to different faults remain in an acceptable range comparing two other control methods. The effectiveness of the proposed control methodology is evaluated qualitatively and quantitatively.

Funding This work is supported by the Smart/Micro Grids Research Center at the University of Kurdistan, Sanandaj, Kurdistan, Iran.

References

1. Hatziargyriou Nikos (2014) Microgrid: architectures and control. Wiley, Hoboken
2. Bevrani H, Francois B, Ise T (2017) Microgrid dynamics and control. Wiley, Hoboken
3. Kundur P, Paserba J, Ajjarapu V et al (2004) Definition and classification of power system stability. IEEE Trans Power Syst 19(3):1387–1401
4. Reddy SS (2017) Optimizing energy and demand response programs using multi-objective optimization. Electr Eng 99(1):397–406
5. Schweppe FC, Tabors RD, Kirtley JL et al (1980) Homeostatic utility control. IEEE Trans Power Appar Syst 99(3):1151–1163
6. Dehghanpour K, Afsharnia S (2015) Electrical demand side contribution to frequency control in power systems: a review on technical aspects. Renew Sustain Energy Rev 41:1267–1276
7. Doğan A, Alçı M (2018) Real-time demand response of thermostatic load with active control. Electr Eng 100(4):2649–2658
8. Shareef H, Ahmed MS, Mohamed A, Al Hassan E (2018) Review on home energy management system considering demand responses, smart technologies, and intelligent controllers. IEEE Access 6:24498–24509
9. Deng R, Yang Z, Chow MY, Chen J (2015) A survey on demand response in smart grids: mathematical models and approaches. IEEE Trans Ind Inform 11(3):570–582
10. Guo Y, Pan M, Fang Y (2012) Optimal power management of residential customers in the smart grid. IEEE Trans Parallel Distrib Syst 23(9):1593–1606
11. Pourmousavi SA, Nehrir MH (2014) Introducing dynamic demand response in the LFC model. IEEE Trans Power Syst 29(4):1562–1572
12. Klobasa M (2010) Analysis of demand response and wind integration in Germany's electricity market. IET Renew Power Gener 4(1):55–63
13. Saele H, Grande OS (2011) Demand response from household customers: experiences from a pilot study in Norway. IEEE Trans Smart Grid 2(1):90–97
14. Chuan L, Ukil A (2015) Modeling and validation of electrical load profiling in residential buildings in Singapore. IEEE Trans Power Syst 30(5):2800–2809

15. Vedady Moghadam MR, Ma RTB, Zhang R (2014) Distributed frequency control in smart grids via randomized demand response. IEEE Trans Smart Grid 5(6):2798–2809
16. Pourmousavi SA, Nehrir MH (2012) Real-time central demand response for primary frequency regulation in microgrids. IEEE Trans Smart Grid 3(4):1988–1996
17. Abbasi E (2017) Coordinated primary control reserve by flexible demand and wind power generation. In: 2017 IEEE power & energy society innovative smart grid technologies conference (ISGT), pp 1–5
18. Jiang H, Lin J, Song Y et al (2014) Demand side frequency control scheme in an isolated wind power system for industrial aluminum smelting production. IEEE Trans Power Syst 29(2):844–853
19. Rezaei N, Kalantar M (2015) Stochastic frequency-security constrained energy and reserve management of an inverter interfaced islanded microgrid considering demand response programs. Int J Electr Power Energy Syst 69:273–286
20. Molina-García A, Bouffard F, Kirschen DS (2011) Decentralized demand-side contribution to primary frequency control. IEEE Trans Power Syst 26(1):411–419
21. Gouveia C, Moreira J, Moreira CL, Pecas Lopes JA (2013) Coordinating storage and demand response for microgrid emergency operation. IEEE Trans Smart Grid 4(4):1898–1908
22. Xu Z, Østergaard J, Togeby M (2011) Demand as frequency controlled reserve. IEEE Trans Power Syst 26(3):1062–1071
23. Westermann D, John A (2007) Demand matching wind power generation with wide-area measurement and demand-side management. IEEE Trans Energy Convers 22(1):145–149
24. Huang K-Y, Chin H-C, Huang Y-C (2004) A model reference adaptive control strategy for interruptible load management. IEEE Trans Power Syst 19(1):683–689
25. Navid-Azarbaijani N (1996) Realizing load reduction functions by aperiodic switching of load groups. IEEE Trans Power Syst 11(2):721–727
26. Medina J, Muller N, Roytelman I (2010) Demand response and distribution grid operations: opportunities and challenges. IEEE Trans Smart Grid 1(2):193–198
27. Rezkalla M, Pertl M, Marinelli M (2018) Electric power system inertia: requirements, challenges and solutions. Electr Eng 100(4):2677–2693
28. Rezaei N, Kalantar M (2015) Smart microgrid hierarchical frequency control ancillary service provision based on virtual inertia concept: an integrated demand response and droop controlled distributed generation framework. Energy Convers Manag 92:287–301
29. Bevrani H, Habibi F, Babahajyani P et al (2012) Intelligent frequency control in an AC microgrid: online PSO-based fuzzy tuning approach. IEEE Trans Smart Grid 3(4):1935–1944
30. Shafiee Q, Dragičević T, Vasquez JC, Guerrero JM (2014) Hierarchical control for multiple DC-microgrids clusters. IEEE Trans Energy Convers 29(4):922–933
31. Bevrani H (2014) robust power system frequency control, 2nd edn. Springer, New York
32. Babahajiani P, Shafiee Q, Bevrani H (2018) Intelligent demand response contribution in frequency control of multi-area power systems. IEEE Trans Smart Grid 9(2):1282–1291
33. Zhang L, Good N, Mancarella P (2019) Building-to-grid flexibility: modelling and assessment metrics for residential demand response from heat pump aggregations. Appl Energy 233–234:709–723
34. Morren J, De Haan SWH, Ferreira JA (2006) Contribution of DG units to primary frequency control. Eur Trans Electr Power 16(5):507–521
35. Akkari S, Petit M, Dai J, Guillaud X (2016) Interaction between the voltage-droop and the frequency-droop control for multi-terminal HVDC systems. IET Gener Transm Distrib 10(6):1345–1352
36. Cingoz F, Elrayyah A, Sozer Y (2015) Optimized droop control parameters for effective load sharing and voltage regulation in DC microgrids. Electr Power Compon Syst 43(8–10):879–889
37. De Brabandere K, Bolsens B, Van den Keybus J et al (2007) A voltage and frequency droop control method for parallel inverters. IEEE Trans Power Electron 22(4):1107–1115
38. Sharma R, Suhag S (2019) Virtual impedance based phase locked loop for control of parallel inverters connected to islanded microgrid. Comput Electr Eng 73:58–70
39. Karami A, Mahmoodi Galougahi K (2019) Improvement in power system transient stability by using STATCOM and neural networks. Electr Eng. https://doi.org/10.1007/s00202-019-00753-5
40. Cichocki A, Unbehauen R (1993) Neural networks for optimization and signal processing. Wiley, Hoboken
41. Wu B (1992) An introduction to neural networks and their applications in manufacturing. J Intell Manuf 3(6):391–403
42. Gupta M, Jin L, Homma N (2004) Static and dynamic neural networks: from fundamentals to advanced theory. Wiley, Hoboken
43. Kleineidam G, Krasser M, Reischböck M (2016) The cellular approach: smart energy region Wunsiedel. Testbed for smart grid, smart metering and smart home solutions. Electr Eng 98(4):335–340
44. Bevrani H, Shokoohi S (2013) An intelligent droop control for simultaneous voltage and frequency regulation in Islanded microgrids. IEEE Trans Smart Grid 4(3):1505–1513